Investigation of H atom and free radical behaviour in clathrate hydrates of organic molecules

Mina Mozafari,[a] Lalangi Chandrasena,[a] Iain McKenzie,[a,b] Kerim Samedov,[c] Paul W. Percival,[a,b] *

[a]*Department of Chemistry, Simon Fraser University, Burnaby, BC V5A 1S6, Canada*

[b]*Centre for Molecular and Materials Science, TRIUMF, Vancouver, BC V6T 2A3, Canada*

[c]*Department of Chemistry, University of British Columbia, Vancouver, BC V6T 1Z1, Canada*

15 October 2019

VSI: 16th Tihany

Abstract

Clathrate hydrates are icy materials composed of a lattice of water molecules containing well-defined cavities which can accommodate small guest molecules. Their large storage capacity makes clathrates attractive media for a variety of gas storage and separation applications, but there is relatively little information on the chemical stability and diffusion of guest molecules. At the fundamental level inter-cage transition energies have been calculated, but the results need to be tested with experimental data. Ideally this should involve single-atom transport, using an isotopic tracer or spin label. Muonium (Mu = μ^+e^-) qualifies on both counts. As a single-electron atom with the muon as nucleus it may be considered a light isotope of hydrogen. Furthermore muonium and its reaction products may be monitored by muon spin spectroscopy. In recent years we have used this method to probe H-atom and free radical behaviour in clathrate hydrates. The current work extends studies to benzene and acetone clathrate hydrates. Of note is the simultaneous detection of muonium and muoniated radicals in the same sample. This can happen when Mu is trapped in an empty cavity, remote from its reaction partner. Increase in temperature leads to transport of Mu between cages and results in encounters with reactive guest molecules. By studying the temperature dependence of Mu and radical signals, we have been able to determine the activation energy for transport of Mu between cavities.

Keywords: gas hydrate; clathrate; H atom; free radical; muonium; muon spin spectroscopy

* Corresponding author. Tel.: +1-778-782-4477; e-mail: percival@sfu.ca.

1. Introduction

Clathrate hydrates are crystalline inclusion compounds composed of a lattice of water molecules containing nano-sized cavities which can accommodate small guest molecules (Sloan and Koh, 2007). The best known, methane hydrate, occurs in nature and constitutes a valuable energy resource, exceeding by a factor of two the total of all other petroleum and natural gas reserves in the world (Chong et al., 2016). Clathrate hydrates may also exist on other planetary bodies and play a role in astrophysical and geologic processes (Kargel et al., 1998). The large gas storage properties of clathrate hydrates makes them potential candidates for carbon dioxide capture (Babu et al., 2015) and hydrogen storage (Veluswamy et al., 2014), and the well-defined cage structure could lead to applications in gas separation (Eslamimanesh et al., 2012). Knowledge of the stability, diffusion and reactions of hydrogen atoms and small organic molecules in clathrate hydrates is necessary to assess the viability of these applications. Although matrix isolation is widely used for the study of transient species in frozen inert gases (Bondybey et al., 1999; Feldman et al., 2016) and other solid materials (Feldman 2014), clathrate hydrates provide the opportunity to study isolated guest molecules and their controlled reactions under relatively mild conditions (Koh et al., 2015).

There have been relatively few studies of transient species in clathrate hydrates. Photochemical production is possible (Ceppatelli et al., 2011) but most work involves radiolysis. Free hydrogen atoms have been clearly identified by electron spin resonance (ESR) spectroscopy (Yeon et al., 2008; Shin et al. 2011; Koh et al., 2012) as well as various small alkyl radicals (Takeya et al., 2004, 2005a, 2005b, 2007). Of particular relevance to the current work are studies of H atom transfer from one radical to another (Ohgaki et al., 2008; Kobayashi et al., 2012; Sugahara et al., 2012; Oshima et al. 2014). One disadvantage of radiolysis is its lack of specificity – a variety of transients are produced in the primary events (H, OH, e^-, and others) and their secondary reactions with the clathrate guest can lead to multiple reaction products. Individual ESR spectra are typically gained through careful annealing and selection of appropriate temperatures.

In contrast, our own studies (Percival et al., 2014; Mozafari et al., 2016, 2017, 2018) employ a beam of spin-polarized positive muons (μ^+) which may be stopped in a sample under any desired condition. When the muons thermalize, some of them pick up an electron to form muonium (Mu = μ^+e^-), which can be considered a light isotope of hydrogen ($m_\mu \approx m_p/9$). Thus our experiments are equivalent to suddenly creating a light hydrogen atom in a clathrate cavity and monitoring its behaviour. The detection method, muon spin spectroscopy, permits us to detect, distinguish, and characterize both muonium and its paramagnetic reaction products (muoniated free radicals). Because of the high degree of muon spin polarization typically ~10^8 muons are sufficient for a spectrum. Thus radiation damage is minimal compared with conventional radiolysis. Furthermore, data is collected on the short time-scale dictated by the positive muon lifetime (τ = 2.197 μs), avoiding the complications of subsequent reactions of the primary radical.

Our previous publications describe studies of muonium in clathrate hydrates of cyclopentane and tetrahydrofuran, and muoniated radicals in clathrates of similar unsaturated molecules: cyclopentene, 2,5-dihydrofuran, 2,3,-dihydrofuran, furan, thiophene, pyrrole and isoxazole (Percival et al., 2014; Mozafari et al., 2016, 2018). The current work concerns benzene and acetone hydrates. Figure 1 shows the expected reactions of muonium with these molecules. Although the H atom reacts with acetone by both abstraction and addition, Mu reacts predominantly by addition (Walker, 1998). In any event, abstraction by Mu would result in the diamagnetic molecule MuH, which would not give the characteristic signal of a muoniated radical. The muoniated cyclohexadienyl radical has been studied under a wide variety of conditions: liquid (Roduner et al., 1982), solid (Roduner, 1993), gas-phase (Fleming et al., 1997), in zeolites (Roduner et al., 1998) and on surfaces (Reid et al., 1990), even in superheated water (Percival et al., 2000). The muoniated ketyl radical (2-muoxyprop-2-yl) can also be formed by simple muonium addition, but in this case there is evidence for an alternative ionic route (Hill et al., 1985; Roduner, 1986), as indicated in Fig. 1.

To detect a muoniated radical by means of muon spin rotation (see section 2.2.1) there must be coherent transfer of spin polarization from the incoming muon to the radical. If the mechanism involves muonium then the addition reaction must be very fast (~10^{10} s^{-1}) to avoid spin dephasing in the product. This is because the relevant muon spin precession frequencies in muonium are about an order of magnitude larger than those of the radical. However, if the radical is formed from a diamagnetic state, e.g. the cation formed by muon attachment, the change in precession frequency is much smaller and the requirement for fast reaction is relaxed (Roduner, 1986). A further consequence of the spin-dephasing effect is that muonium and the corresponding radical product cannot be detected simultaneously – if muonium is long-lived enough to detect (> 30 ns) all phase coherence is lost in the product.

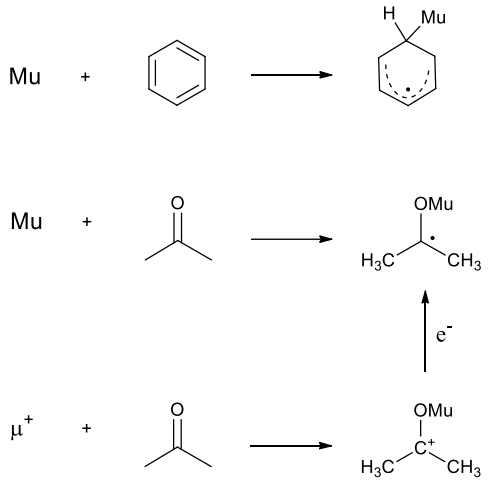

Fig. 1. Reactions of muonium with benzene and acetone and an alternative ionic route to the 2-muoxyprop-2-yl radical.

2. Experimental Methods

2.1. Samples

Acetone hydrate samples were prepared from both normal and deuterated materials (acetone-h6 in H_2O; acetone-d6 in D_2O), using the crushed ice method described previously for furan and dihydrofuran hydrates (Mozafari et al., 2016). The molar ratio of organic to water was 1:17, which corresponds to one guest molecule for each $5^{12}6^4$ cavity of the type-II clathrate structure. It is assumed that the smaller (5^{12}) cavities were empty, although there is a possibility that some contained molecular nitrogen since all operations were carried out in a nitrogen atmosphere.

The benzene hydrate samples were also structure II clathrates, with benzene occupying the $5^{12}6^4$ cavities, but with methane or xenon in the 5^{12} cavities. These double hydrates were also prepared by the crushed ice method, but in this case the mixture was cooled under gas pressure (methane or xenon), as described for pyrrole-methane and thiophene-xenon (Mozafari , 2017; Mozafari et al., 2018).

All samples were crushed to a fine powder before being sealed in stainless-steel sample cells for the μSR experiments.

2.2. Muon spin spectroscopy

Muon spin spectroscopy (μSR) experiments were carried out at the TRIUMF accelerator facility, using spin-polarized positive muons from the M15 and M20 beam lines. Two types of spectrum were acquired: transverse-field muon spin rotation (TF-μSR) and muon avoided level-crossing resonance (μLCR). Basic descriptions and technical details can be found in earlier publications (Percival et al., 1999; West and Percival, 2010; Percival et al., 2014); the sections below are provided to explain how hyperfine constants are extracted from the spectra.

2.2.1. Muon spin rotation

The TF-μSR technique is used to detect muon spin precession frequencies. Muons incorporated in diamagnetic molecules (e.g. MuH, MuOH) precess at the muon Larmor frequency $\nu_\mu = \gamma_\mu B$, where $\nu_\mu = 13.554$ MHz/G and B is the magnetic field strength (in G). Approximately 60% of the muons form diamagnetic species in our hydrate materials, so ν_μ is a dominant feature of all TF-μSR spectra.

Muons in the form of muonium atoms exhibit four precession frequencies but two of them are too high to be resolved by our apparatus. The other two, ν_{12} and ν_{23}, are degenerate at zero field but have a splitting that increases with magnetic field and depends on the muon-electron hyperfine constant. The isotropic hfc can be calculated from ν_μ, ν_{12} and ν_{23}:

$$A_0 = 2\left[\frac{(\nu_{23}+\nu_\mu)(\nu_{12}+\nu_\mu)}{\nu_{23}-\nu_{12}}\right]. \quad (1)$$

Muoniated free radicals typically have additional precession frequencies as a result of other nuclear-electron hyperfine interactions. However, at sufficiently high field the frequencies form two groups, roughly equidistant from the diamagnetic frequency:

$$\nu_{R1} = \nu_m - \tfrac{1}{2}A_\mu \quad (2)$$

$$\nu_{R2} = \nu_m + \tfrac{1}{2}A_\mu \quad (3)$$

where ν_m depends on the muon hyperfine constant, A_μ, and the electron Larmor frequency, ν_e:

$$\nu_m = \left[\sqrt{A_\mu^2 + (\nu_e+\nu_\mu)^2} - \nu_e + \nu_\mu\right]/2 \quad (4)$$

A_μ is given by the difference of the two radical precession frequencies

$$A_\mu = \nu_{R2} - \nu_{R1} \quad (5)$$

but it can also be calculated from one of those radical frequencies and the diamagnetic frequency:

$$A_\mu = 2\frac{(\nu_\mu - \nu_{R1})(\nu_e + \nu_{R1})}{\nu_e - \nu_\mu + 2\nu_{R1}}. \quad (6)$$

Although TF-μSR spectra are usually displayed as Fourier transforms, the original data are collected as time histograms (West and Percival, 2010). Accordingly, quantitative fits are carried out in time space.

2.2.2. Muon avoided level-crossing resonance

μLCR involves sweeping the applied magnetic field while monitoring the muon spin polarization. Since the muon spins are initially aligned parallel to the field nothing happens until there is a mixing of spin levels which

results in loss of muon polarization. There are two types of LCR relevant to this work. One is due to a "flip-flop" simultaneous transition of a muon and a proton spin; the magnetic field at resonance is given by

$$B_{\Delta M=0} = \frac{1}{2}\left[\frac{(A_\mu - A_p)}{(\gamma_\mu - \gamma_p)} - \frac{(A_\mu + A_p)}{\gamma_e}\right] \tag{7}$$

where γ_p and A_p are the gyromagnetic ratio and hyperfine constant of the proton. The second type of resonance involves only a muon spin (hence $\Delta M = 1$, where M is the z-component of the total electron-muon-proton spin). It only occurs when there is some additional interaction (here hyperfine anisotropy). The resonance field is directly proportional to the muon hfc:

$$B_{\Delta M=1} = \frac{1}{2} A_\mu \left[\frac{1}{\gamma_\mu} - \frac{1}{\gamma_e}\right]. \tag{8}$$

3. Benzene clathrate Hydrates

Characteristic muonium precession frequencies are clearly seen in the TF-μSR spectrum obtained from a sample of benzene-methane hydrate at 235 K (Fig. 2). Combining these frequencies (243.95 ± 0.05 MHz and 274.40 ± 0.06 MHz) with the muon Larmor frequency (2.523 MHz) leads (Eq. 1) to the hyperfine constant A_{Mu} = 4483 ± 32 MHz. As noted for other clathrate hydrates (Percival et al., 2014) this is close to the vacuum value, consistent with unbound muonium in an otherwise empty cavity. The sharpness of the spectral peaks indicates lack of reaction (on the microsecond time-scale dictated by muon decay). It was therefore a surprise when we detected the unmistakable signal of a muoniated radical in a spectrum taken from the same sample at higher magnetic field (Fig. 3). In addition to the radical precession frequency at ν_{R1} = -155.81± 0.06 MHz there is a weaker one at ν_{R2} = 371.36 MHz (not shown in Fig. 3). Applying Eq. (6), with ν_μ = 104.533 MHz, leads to A_μ = 527.1 ± 0.1 MHz. This is close to literature values for the muoniated cyclohexadienyl radical in liquid benzene (Roduner et al., 1982), solid benzene (Roduner, 1993) and the gas phase (Fleming et al., 1997), given the well-established negative temperature dependence of the muon hfc (Yu et al., 1990).

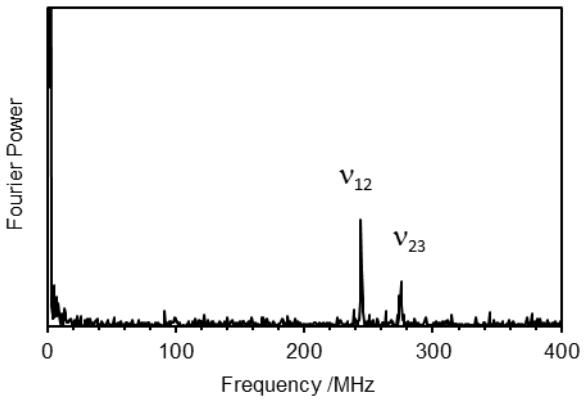

Fig. 2. Fourier power TF-μSR spectrum at 186 G obtained from benzene-methane hydrate at 235 K. ν_{12} and ν_{23} are muonium precession frequencies. The intense diamagnetic signal is at 2.5 MHz and not resolved in this display.

TF-μSR measurements at other temperatures confirmed the negative temperature dependence of A_μ. A similar temperature effect was also noted for the methylene (CHMu) proton hfc, which was determined from the $\Delta M = 0$ LCR (Fig. 4). In contrast to the symmetrical shape of the $\Delta M = 0$ resonance, the $\Delta M = 1$ resonance exhibits the characteristic "powder-pattern" shape indicative of anisotropy (Fig. 5).

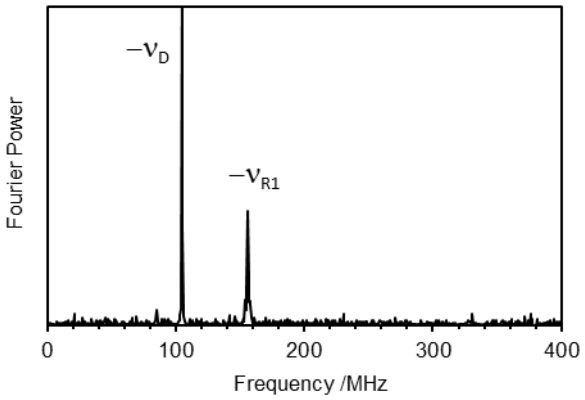

Fig. 3. Negative frequency portion of the Fourier power TF-μSR spectrum at 7.712 kG obtained from benzene-methane hydrate at 235 K.

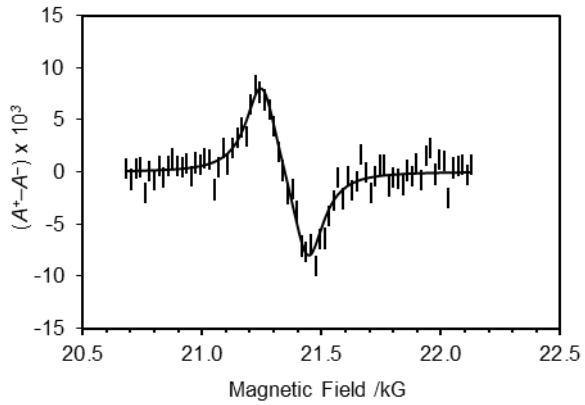

Fig. 4. Portion of the μLCR spectrum obtained from benzene-methane hydrate at 235 K. This displays the $\Delta M = 0$ resonance assigned to the CHMu group. The differential shape is a consequence of square-wave field modulation at ±96 G.

Both TF-μSR and μLCR spectra showed changes in signal amplitudes with temperature: the radical intensity increases and muonium falls with temperature. However, in view of the relatively weak signals and limits on muon beam time a full quantitative study was not attempted. Instead this was undertaken with acetone clathrate hydrate, which gives stronger signals and is easier to prepare.

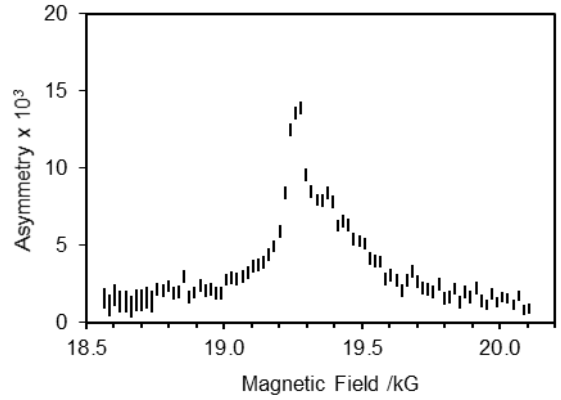

Fig. 5. Portion of the μLCR spectrum obtained from benzene-methane hydrate at 235 K. This displays the $\Delta M = 1$ resonance displayed in integral form.

4. Acetone clathrate hydrates

A TF-μSR spectrum obtained from acetone-d6/D_2O hydrate is shown in Fig. 6. It is remarkable in displaying in a single spectrum signals from both muonium and a muoniated radical. However, the muon hfc of the radical is so small (~30 MHz) that the two precession frequencies are not well resolved from the diamagnetic peak at 1.42 MHz. Spectra taken at higher magnetic field give clearer displays of the radical precession signals; an example is shown in Fig. 7. Protiated samples were also studied, but the signals are broader and less well-resolved.

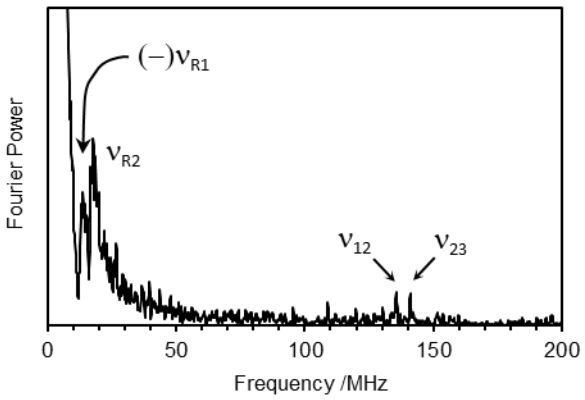

Fig. 6. Fourier power TF-μSR spectrum at 105 G obtained from acetone-d6/D_2O hydrate at 180 K.

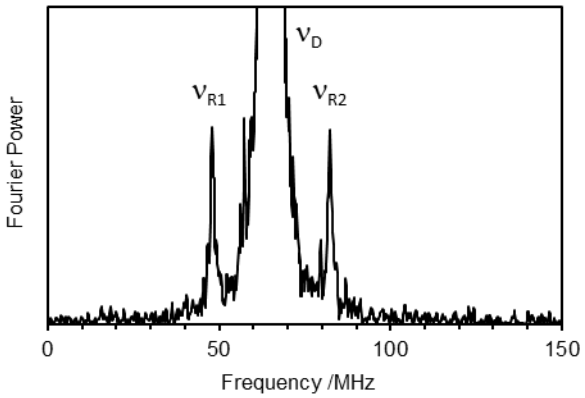

Fig. 7. Fourier power TF-μSR spectrum at 4.712 kG obtained from acetone-d6/D_2O hydrate at 250 K.

The small muon hfc (34.6 MHz from the spectrum shown in Fig. 7) is consistent with expectations for the 2-muoxyprop-2-yl radical. To confirm the assignment we undertook μLCR studies. With the reasonable expectation that the methyl groups act as free rotors, the six protons (or deuterons) should be equivalent and their hyperfine constants essentially temperature-independent, with a proton hfc value close to 60 MHz (Percival et al., 2005). Applying Eq. (7) leads to the prediction that there should be a $\Delta M = 0$ resonance at about (-)1.2 kG (depending on the temperature-dependent value of A_μ). The expected signal was indeed observed, but with a somewhat distorted line shape. The distortion is explained by the close degeneracy of the $\Delta M = 0$ and $\Delta M = 1$ resonances, which is only possible here because $A_p > A_\mu$. The separation between the two resonances increases at lower temperatures and the two signals are partially resolved in the example shown in Fig. 8. Both resonances were also observed for the acetone-d6/D_2O hydrate, but in this case the $\Delta M = 0$ resonance appears below $\Delta M = 1$ and is considerably weaker, due to the smaller deuteron hfc.

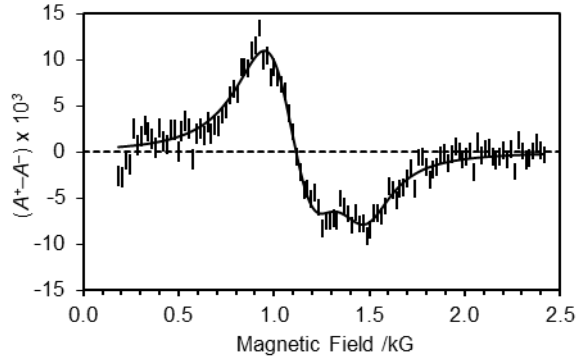

Fig. 8. μLCR spectrum obtained from acetone-h6/H_2O hydrate at 180 K.

Figure 9 compares the muon hfcs determined from the $\Delta M = 1$ resonance (using eq. (8)) to those determined from the TF-μSR spectra. There is no significant difference between normal and perdeuterated samples and for the two spectroscopic methods. This agreement also supports our interpretation of the spectrum shown in Fig. 8 – the $\Delta M = 1$ resonance lies below the $\Delta M = 0$ resonance. The proton hfc deduced from the latter (using Eq. (7)) is 55.4 MHz, in good agreement with the value determined for the same radical in liquid acetone: 55.1 MHz (Heming et al., 1986).

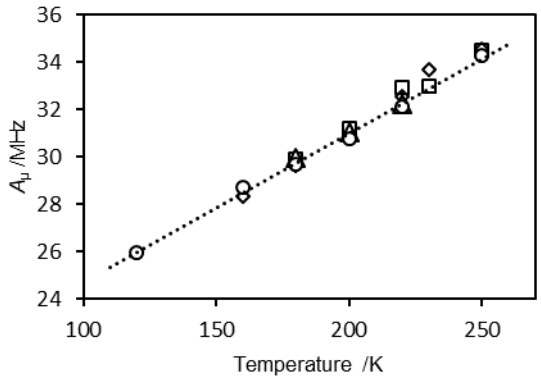

Fig. 9. Muon hyperfine constants for the radical detected by TF-μSR in acetone-h6/H_2O hydrate (squares), TF-μSR in acetone-d6/D_2O hydrate (diamonds), μLCR in acetone-h6/H_2O hydrate (triangles), and μLCR in acetone-d6/D_2O hydrate (circles). The dotted line is a straight line fit to the data set denoted by circles.

Figure 10 compares the temperature dependence of the muon hfc for the enclathrated radical with literature data for the 2-muoxy-prop-2-yl radical in liquid solution (Buttar et al., 1990; Ghandi et al., 2003). The temperature dependence of the liquid-phase data has been ascribed to vibrational averaging of torsional motion about the Ċ-O bond, and the solvent effect (pure acetone vs. aqueous solution) to hydrogen bonding (Buttar et al., 1990). The marked contrast between the clathrate data and the solution data supports the notion that hydrogen-bonding impedes the torsional motion in solution. The torsional barrier is smaller for the radical in the clathrate, and consequently the muon hfc has reduced temperature-dependence. Buttar et al. (1990) have also suggested an additional effect involving partial transfer of unpaired spin density from the carbon to oxygen. This is equivalent to increasing the participation of an ionic resonance structure for the radical: $(CH_3)_2\dot{C}–OMu \leftrightarrow (CH_3)_2C^{-}–O^{\cdot+}Mu$, something a polar solvent would promote. Unpaired spin density at the oxygen gives a negative contribution to the spin density at the muon, hence reducing the overall hfc.

The intensity of the radical signals as measured from the TF-μSR spectrum was found to vary in sinusoidal manner with a delay in the start of the Fourier transform window. The spectrum in Fig. 7 was obtained by transforming 2 μs of time data delayed 44 ns after muon injection. This curious effect has been noted by us in a variety of radicals but only briefly documented in the literature (West and Percival, 2010). A common feature is the polar nature of the reactants, which leads us to suspect the involvement of an ionic mechanism for formation of the radical. We suggest muon attachment followed by reaction with an excess electron, as indicated in Fig. 1. An alternative is initial formation of the acetone radical anion, $(CH_3)_2\dot{C}–O^{-}$, followed by reaction with Mu^+ (Hill et al., 1985; Roduner, 1986). The muon species is written as Mu^+ rather than μ^+ to emphasize that it is not a free muon but attached to acetone or water. Of course the same could be said of e^- (Fig. 1), so perhaps the best description for the reactions in pure acetone and aqueous solution would be (Hill et al., 1985):

$$(CH_3)_2\dot{C}–O^{-} + (CH_3)_2C^{+}–OMu \rightarrow (CH_3)_2\dot{C}–OMu + (CH_3)_2C{=}O \quad (9)$$

$$(CH_3)_2\dot{C}–O^{-} + H_2OMu^{+} \rightarrow (CH_3)_2\dot{C}–OMu + H_2O \quad (10)$$

The lifetime of Mu+ in liquid acetone has been estimated to be 3 ns, suggesting that the muon is thermalized about 3–4 nm from the closest spur electron (Roduner, 1986).

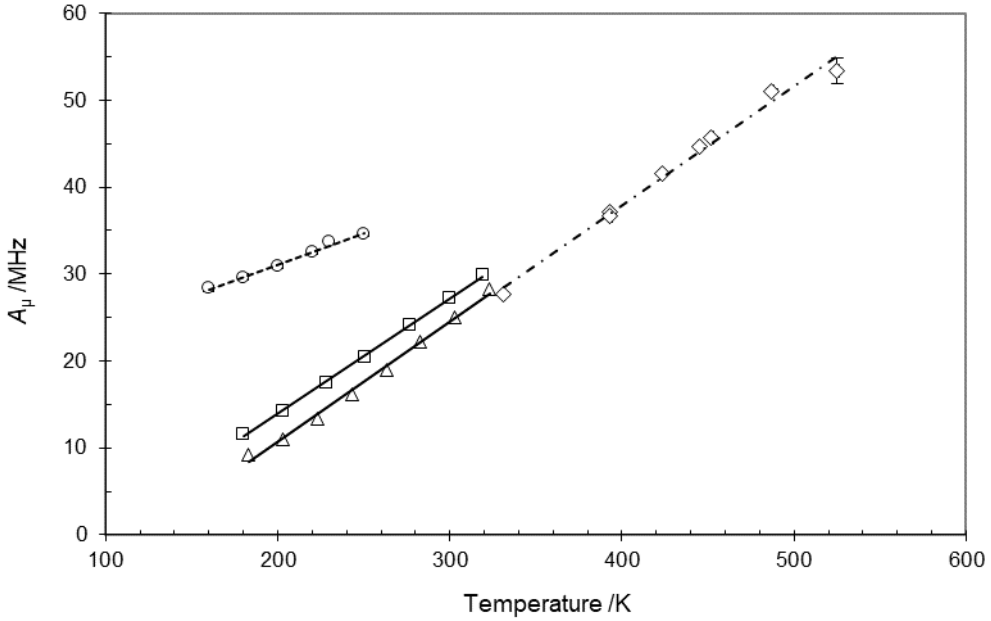

Fig. 10. Muon hyperfine constants for the muoxy-prop-2-yl radical detected in acetone-d6/D_2O hydrate (circles), compared with literature data for the radical in pure acetone (squares, Buttar et al., 1990), in a 20:1 mixture of acetone: water (triangles, Buttar et al., 1990), and in hot pressurized water (diamonds, Ghandi et al. 2003). Each data set is displayed with its own straight-line fit.

Regardless of the ionic route discussed above, the direct detection of muonium by TF-μSR (Fig. 6) and its disappearance at higher temperature shows that the radical can also be formed by direct Mu addition. If Mu is trapped in an empty cage at low temperature it could react with acetone in a neighbouring cage when it becomes mobile. To investigate this we measured the amplitude of the radical signal as a function of temperature, using the $\Delta M = 1$ LCR signal to avoid the complications of loss of phase coherence in transverse field. It is assumed here that the signal amplitude at each temperature is directly proportional to the yield of the radical. This is not always so, as LCR intensities can depend on radical dynamics (Tregenna-Piggott, 1996). However, in the relevant range of temperature there was no evidence of asymmetric line shapes or large changes of symmetric linewidth associated with reorientational dynamics. We therefore discount this possibility for the relatively sudden change in signal amplitude observed in the region of 200 K.

The results are shown in Figure 11. The data suggest that 76% of the radicals are formed promptly, perhaps partly by the ionic mechanism, and that the remaining 24% form by a slower activated process. The line through the points represents a simple model for activated diffusion of Mu from one potential well to another, as described by the function $A\exp(-T_c/T)/[1+A\exp(-T_c/T)]$. The characteristic temperature, T_c = 3098 K, corresponds to an activation energy of 25.8 kJ mol^{-1}.

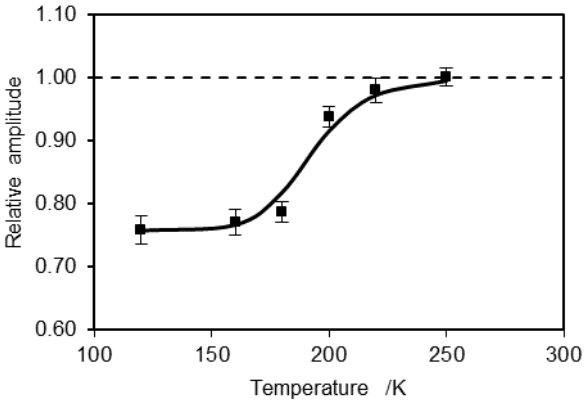

Fig. 11. Relative amplitude of the $(CD_3)_2\dot{C}OMu$ radical in acetone-d6/D_2O hydrate, as determined from the ΔM = 1 μLCR signal. The solid line is a fit of the function $A\exp(-T_c/T)/[1+A\exp(-T_c/T)]$ to the temperature-dependent component.

Our results may be compared with experimental and computational data for H atoms. Yeon et al. (2008) used NMR to study the migration of H atoms in tetrahydrofuran-H_2 double clathrate hydrate, and concluded that H becomes mobile above 180 K. Alavi and Ripmeester (2009) calculated the energy barriers for H atom migration through pentagonal and hexagonal faces of small and large cages of a structure II clathrate. They included tunneling corrections but not zero-point energy, which they argue would increase the effective migration barrier due to transverse vibrational modes at the window between cages. Thus their value of ~17 kJ mol^{-1} for H migration through the large hexagonal face should be considered a lower estimate. There are even larger zero-vibrational contributions for Mu, so our value for the activation energy is consistent with the H atom calculation. A similar isotope effect at the "bottleneck" has previously been invoked to explain faster diffusion of D atoms than H in ice-Ih (Bartels et al., 1992).

It is also interesting to compare diffusion of H and Mu through clathrates with diffusion through liquid water, if only because early molecular dynamics studies suggested the existence of a transient clathrate-like cage of water molecules about the free atoms (Tse and Klein, 1983; Raedt et al., 1984). Recent experimental studies of spin-exchange rates show that Mu diffuses faster than H, but the activation energies are very similar and close to 15 kJ mol^{-1} (Walker et al., 2016). The detailed results are in good accord with the molecular dynamics study by Markland et al (2008), which showed that diffusion involves both hopping of the atom between cavities, and diffusion of the cavities in the liquid. The former mechanism is mass-dependent but the latter not. In ice (and similarly in clathrate hydrates) intercavity hopping is the only option. It was concluded that quantum effects are critical for an accurate description of the diffusion of these light atoms.

5. Conclusions

Atomic muonium has been detected in benzene and acetone clathrate hydrates. The muon hyperfine constant is close to the vacuum value, showing that Mu is unbound, similar to endohedral Mu in fullerene C_{60} (Ansaldo et al., 1992) and C_{70} (Niedermayer et al., 1993) and in silasesquioxane cages (Dilger et al., 2000). Muoniated radicals have also been detected in the benzene and acetone clathrates. The simultaneous observation of Mu and its radical products has been previously noted only for fullerenes (Percival and Wlodek, 1992; Niedermayer et al., 1993), where Mu is unreactive inside the cage but forms radicals by reaction on the outside surface. In the case of clathrates, which have a continuous structure of interlocking polyhedrons, the radicals must be *inside* the cavities.

The muoniated cyclohexadienyl radical detected in benzene clathrates has a muon hyperfine constant close to the values measured in other media, suggesting that the clathrate cage has little effect. In contrast, there is a significant difference for the muoniated ketyl radical formed in the acetone clathrates and in liquid solution. On the other hand, there is NMR evidence that acetone experiences less hydrogen-bonding to the cage wall in the clathrate than it does in solution (Takebayashi et al., 2002). Thus the muoniated radical in the clathrate is not as affected by the medium as first thought.

A significant difference between the muoniated cyclohexadienyl and ketyl radicals is in their mode of formation. Delayed formation of the latter supports the view that some of the radicals are formed via an ionic mechanism, i.e. reaction of muonated acetone (a diamagnetic species) with the acetone radical anion. Despite this alternative pathway it is evident that a fraction of radicals is formed by simple addition of Mu to acetone. The temperature-dependence of the radical yield is consistent with an activated process for Mu transport – a Mu atom forms in an empty cage and must pass through a "bottleneck" window to an occupied cavity where it can react.

Acknowledgements

We thank Dr. Jean-Claude Brodovitch for assistance with the muon experiments, and the staff of the Centre for Molecular and Materials Science at TRIUMF for technical support. We are grateful to Dr. John Ripmeester for helpful advice on the preparation and characterization of clathrates. This work was financially supported by the Natural Sciences and Engineering Research Council of Canada and Simon Fraser University. TRIUMF is operated by a consortium of Canadian universities, and receives federal funding via a contribution agreement with the National Research Council of Canada.

References

Alavi, S., Ripmeester, J.A., 2009. Migration of hydrogen radicals through clathrate hydrate cages. Chem. Phys. Lett. 479, 234-237. https://doi.org/10.1016/j.cplett.2009.08.044.

Ansaldo, E.J., Boyle, J., Niedermayer, C., Morris, G.D., Brewer, J.H., Stronach, C.E., Cary, R.S., 1992. Formation of Muonium and a Muonic Radical in Fullerene. Z. Phys. B-Condens. Mat. 86, 317-318. https://doi.org/10.1007/bf01323722.

Babu, P., Linga, P., Kumar, R., Englezos, P., 2015. A review of the hydrate based gas separation (HBGS) process for carbon dioxide pre-combustion capture. Energy 85, 261-279. https://doi.org/10.1016/j.energy.2015.03.103.

Bartels, D.M., Han, P., Percival, P.W., 1992. Diffusion and CIDEP of H and D atoms in solid H_2O, D_2O and isotopic mixtures. Chem. Phys. 164, 421-437. https://doi.org/10.1016/0301-0104(92)87079-O.

Bondybey, V. E., Räsänen, M., Lammers, A., 1999. Chapter 10. Rare-gas matrices, their photochemistry and dynamics: recent advances in selected areas. Annu. Rep. Sect. C Phys. Chem. 95, 331-372. https://doi.org/10.1039/PC095331.

Buttar, D., Macrae, R.M., Webster, B.C., Roduner, E., 1990. Solvent Effects on the Hyperfine Coupling-Constant and Barrier to Internal-Rotation for the 2-Muoxyprop-2-yl Radical. Hyperfine Interact. 65, 927-936. https://doi.org/10.1007/BF02397744.

Ceppatelli, M., Bini, R., Schettino, V., 2011. High-pressure reactivity of clathrate hydrates by two-photon dissociation of water. Phys. Chem. Chem. Phys. 13, 1264-1275. https://doi.org/10.1039/c0cp01318h.

Chong, Z.R., Yang, S.H.B., Babu, P., Linga, P., Li, X.-S., 2016. Review of natural gas hydrates as an energy resource: Prospects and challenges. Applied Energy 162, 1633-1652. https://doi.org/10.1016/j.apenergy.2014.12.061.

Dilger, H., Roduner, E., Scheuermann, R., Major, J., Schefzik, M., Stosser, R., Pach, M., Fleming, D.G., 2000. Mass and temperature effects on the hyperfine coupling of atomic hydrogen isotopes in cages. Physica B 289, 482-486. https://doi.org/10.1016/s0921-4526(00)00441-5.

Eslamimanesh, A., Mohammadi, A.H., Richon, D., Naidoo, P., Ramjugernath, D., 2012. Application of gas hydrate formation in separation processes: A review of experimental studies. J. Chem. Thermodyn. 46, 62-71. http://dx.doi.org/10.1016/j.jct.2011.10.006.

Feldman, V.I., 2014. EPR and IR Spectroscopy of Free Radicals and Radical Ions Produced by Radiation in Solid Systems, in: Lund, A., Shiotani, M. (Eds.), Applications of EPR in Radiation Research. Springer International Publishing, Cham, pp. 151-187. https://doi.org/10.1007/978-3-319-09216-4_5.

Feldman, V.I., Ryazantsev, S.V., Saenko, E.V., Kameneva, S.V., Shiryaeva, E.S., 2016. Matrix isolation model studies on the radiation-induced transformations of small molecules of astrochemical and atmospheric interest. Radiat. Phys. Chem. 124, 7-13. https://doi.org/10.1016/j.radphyschem.2015.12.005.

Fleming, D.G., Arseneau, D.J., Pan, J.J., Shelley, M.Y., Senba, M., Percival, P.W., 1997. Hyperfine coupling constants of muonium-substituted cyclohexadienyl radicals in the gas phase: C_6H_6Mu, C_6D_6Mu, C_6F_6Mu. Appl. Mag. Reson. 13, 181-194. https://doi.org/10.1007/BF03161980.

Ghandi, K., Addison-Jones, B., Brodovitch, J.C., McCollum, B.M., McKenzie, L., Percival, P.W., 2003. Enolization of acetone in superheated water detected via radical formation. J. Am. Chem. Soc. 125, 9594-9595. https://doi.org/10.1021/ja036377x.

Heming, M., Roduner, E., Patterson, B.D., Odermatt, W., Schneider, J., Baumeler, H., Keller, H., Savic, I.M., 1986. Detection of Muonated Free Radicals through the Effects of Avoided Level-Crossing. Theory and Analysis of Spectra. Chem. Phys. Lett. 128, 100-106. https://doi.org/10.1016/0009-2614(86)80154-3.

Hill, A., Symons, M.C.R., Cox, S.F.J., de Renzi, R., Scott, C.A., Bucci, C., Vecli, A., 1985. Studies of muonium-substituted molecules in propan-2-one and in aqueous solutions of propan-2-one. J. Chem. Soc., Faraday Trans. 1, 81, 433-448. https://doi.org/10.1039/f19858100433.

Kargel J.S., Lunine J.I., 1998. Clathrate Hydrates on Earth and in the Solar System. In: Schmitt B., De Bergh C., Festou M. (eds) Solar System Ices. Astrophysics and Space Science Library, vol 227. Springer, Dordrecht. https://doi.org/10.1007/978-94-011-5252-5_5.

Kobayashi, N., Minami, T., Tani, A., Nakagoshi, M., Sugahara, T., Takeya, K., Ohgaki, K., 2012. Intermolecular Hydrogen Transfer in Isobutane Hydrate. Energies 5, 1705-1712. https://doi.org/10.3390/en5061705.

Koh, D.Y., Kang, H., Park, J., Shin, W., Lee, H., 2012. Atomic Hydrogen Production from Semi-clathrate Hydrates. J. Am. Chem. Soc. 134, 5560-5562. https://doi.org/10.1021/ja300567b.

Koh, D.Y., Kang, H., Lee, H., 2015. Reactive radical cation transfer in the cages of icy clathrate hydrates. Korean J. Chem. Eng. 32, 350-353. https://doi.org/10.1007/s11814-014-0280-3.

Markland, T.E., Habershon, S., Manolopoulos, D.E., 2008. Quantum diffusion of hydrogen and muonium atoms in liquid water and hexagonal ice. J. Chem. Phys. 128, 194506. https://doi.org/10.1063/1.2925792.

Mozafari, M., Brodovitch, J.C., Chandrasena, L., Percival, P.W., 2016. Characterization of Free Radicals in Clathrate Hydrates of Furan, 2,3-Dihydrofuran, and 2,5-Dihydrofuran by Muon Spin Spectroscopy. J. Phys. Chem. A 120, 8521-8528. https://doi.org/ 10.1021/acs.jpca.6b08653.

Mozafari, M., 2017. Ph. D. Thesis, Simon Fraser University.

Mozafari, M., Chandrasena, L., McKenzie, I., Samedov, K., Percival, P.W., 2018. Characterization of free radicals in clathrate hydrates of pyrrole, thiophene, and isoxazole by muon spin spectroscopy. Can. J. Chem. 96, 217-225. https://doi.org/10.1139/cjc-2017-0313.

Niedermayer, C., Reid, I.D., Roduner, E., Ansaldo, E.J., Bernhard, C., Binninger, U., Gluckler, H., Recknagel, E., Budnick, J.I., Weidinger, A., 1993. Simultaneous Observation of Muonium and Multiple Free-Radicals in Muon-Implanted C-70. Phys. Rev. B 47, 10923-10926. https://doi.org/10.1103/PhysRevB.47.10923.

Ohgaki, K., Nakatsuji, K., Takeya, K., Tani, A., Sugahara, T., 2008. Hydrogen transfer from guest molecule to radical in adjacent hydrate-cages. Phys. Chem. Chem. Phys. 10, 80-82. https://doi.org/10.1039/b715284a.

Oshima, M., Tani, A., Sugahara, T., Kitano, K., Ohgaki, K., 2014. Reactions of HOCO radicals through hydrogen-atom hopping utilizing clathrate hydrates as an observational matrix. Phys. Chem. Chem. Phys. 16, 3792-3797. https://doi.org/ 10.1039/c3cp54680b.

Percival, P.W., Wlodek, S., 1992. The structure of $C_{60}Mu$ and other fullerenyl radicals. Chem. Phys. Lett. 196, 317-320. https://doi.org/10.1016/0009-2614(92)85974-F.

Percival, P.W., Addison-Jones, B., Brodovitch, J.C., Ghandi, K., Schuth, J., 1999. Free radicals formed by H(Mu) addition to pyrene. Can. J. Chem. 77, 326-331. https://doi.org/10.1139/v99-031.

Percival, P.W., Ghandi, K., Brodovitch, J.C., Addison-Jones, B., McKenzie, I., 2000. Detection of muoniated organic free radicals in supercritical water. Phys. Chem. Chem. Phys. 2, 4717-4720. https://doi.org/10.1039/b005762m.

Percival, P.W., Brodovitch, J.C., Ghandi, K., McCollum, B.M., McKenzie, I., 2005. Organic Free Radicals in Superheated Water Studied by Muon Spin Spectroscopy. J. Am. Chem. Soc. 127, 13714-13719. https://doi.org/10.1021/ja0537070.

Percival, P.W., Mozafari, M., Brodovitch, J.C., Chandrasena, L., 2014. Organic Free Radicals in Clathrate Hydrates Investigated by Muon Spin Spectroscopy. J. Phys. Chem. A 118, 1162-1167. https://doi.org/10.1021/jp411297s.

Raedt, B.D., Sprik, M., Klein, M.L., 1984. Computer simulation of muonium in water. The Journal of Chemical Physics 80, 5719-5724. https://doi.org/10.1063/1.446641.

Reid, I.D., Azuma, T., Roduner, E., 1990. Surface-adsorbed free radicals observed by positive-muon avoided-level-crossing resonance. Nature 345, 328-330. https://doi.org/10.1038/345328a0.

Roduner, E., Brinkman, G.A., Louwrier, P.W.F., 1982. Muonium-Substituted Organic Free-Radicals in Liquids - Muon Electron Hyperfine Coupling-Constants and the Selectivity of Formation of Methyl-Substituted and Fluorine-Substituted Cyclohexadienyl-Type Radicals. Chem. Phys. 73, 117-130. https://doi.org/10.1016/0301-0104(82)85154-9.

Roduner, E., 1986. End-of-Track Radiolytical Processes and Radical Formation in Positive Muon Irradiated Acetone. Radiat. Phys. Chem. 28, 75-84. https://doi.org/10.1016/1359-0197(86)90040-8

Roduner, E., 1993. Polarized positive muons probing free-radicals - a variant of magnetic-resonance. Chem. Soc. Rev. 22, 337-346. https://doi.org/10.1039/CS9932200337.

Roduner, E., Stolmar, M., Dilger, H., Reid, I.D., 1998. Reorientational dynamics of cyclohexadienyl radicals in high-silica ZSM-5. J. Phys. Chem. A 102, 7591-7597. https://doi.org/10.1021/jp982691f.

Shin, K., Cha, M., Kim, H., Jung, Y., Kang, Y.S., Lee, H., 2011. Direct observation of atomic hydrogen generated from the water framework of clathrate hydrates. Chem. Commun. 47, 674-676. https://doi.org/10.1039/c0cc02616f.

Sloan, E.D., Koh, C.A., 2007. Clathrate Hydrates of Natural Gases, third ed. CRC Press, Boca Raton. https://doi.org/10.1201/9781420008494.

Sugahara, T., Kobayashi, Y., Tani, A., Inoue, T., Ohgaki, K., 2012. Intermolecular Hydrogen Transfer between Guest Species in Small and Large Cages of Methane plus Propane Mixed Gas Hydrates. J. Phys. Chem. A 116, 2405-2408. https://doi.org/10.1021/jp300814s.

Takebayashi, Y., Otake, K., 2002. Molecular Interactions and Rotational Dynamics in Clathrate Hydrate. Rev. High Press. Sci. Techno. 12, 22-27. (In Japanese) https://doi.org/10.4131/jshpreview.12.22.

Takeya, K., Tani, A., Yada, T., Ikeya, M., Ohgaki, K., 2004. Electron spin resonance study on gamma-ray-induced methyl radicals in methane hydrates. Jpn. J. Appl. Phys. 43, 353-357. https://doi.org/10.1143/jjap.43.353.

Takeya, K., Nango, K., Sugahara, T., Ohgaki, K., Tani, A., 2005. Activation Energy of Methyl Radical Decay in Methane Hydrate. J. Phys. Chem. B 109, 21086-21088. https://doi.org/10.1021/jp054028e.

Takeya, K., Tani, A., Yada, T., Ikeya, M., 2005. ESR investigation of γ-irradiated natural methane hydrate from Blake Ridge Diapir, off east North America in ODP Leg 164. Appl. Radiat. Isotopes 62, 371-374. https://doi.org/10.1016/j.apradiso.2004.08.021.

Takeya, K., Sugahara, T., Ohgaki, K., Tani, A., 2007. Electron spin resonance study on gamma-ray-induced radical species in ethylene hydrate. Radiat. Meas. 42, 1301-1306. https://doi.org/10.1016/j.radmeas.2007.07.001.

Tregenna-Piggott, P.L.W., Roduner, E., Santos, S., 1996. Calculation of the avoided level-crossing muon spin resonance response for various stochastic motions using Monte Carlo methods. Chem. Phys. 203, 317-337. https://doi.org/10.1016/0301-0104(95)00385-1.

Tse, J.S., Klein, M.L., 1983. Are hydrogen atoms solvated by water molecules? The Journal of Physical Chemistry 87, 5055-5057. https://doi.org/10.1021/j150643a002.

Veluswamy, H.P., Kumar, R., Linga, P., 2014. Hydrogen storage in clathrate hydrates: Current state of the art and future directions. Applied Energy 122, 112-132. http://doi.org/10.1016/j.apenergy.2014.01.063.

Walker, D.C., 1998. Kinetic isotope effects in solution reactions of muonium atoms as H-isotopes. J. Chem. Soc.-Faraday Trans. 94, 1-9. https://doi.org/10.1039/A706375J.

Walker, J.A., Mezyk, S.P., Roduner, E., Bartels, D.M., 2016. Isotope Dependence and Quantum Effects on Atomic Hydrogen Diffusion in Liquid Water. J. Phys. Chem. B 120, 1771-1779. https://doi.org/10.1021/acs.jpcb.5b09375.

West, R., Percival, P.W., 2010. Organosilicon compounds meet subatomic physics: Muon spin resonance. Dalton Trans. 39, 9209-9216. https://doi.org/10.1039/C0DT00188K.

Yeon, S.H., Seol, J., Park, Y., Koh, D.Y., Kang, Y.S., Lee, H., 2008. Spectroscopic observation of atomic hydrogen radicals entrapped in icy hydrogen hydrate. J. Am. Chem. Soc. 130, 9208-9209. https://doi.org/10.1021/ja802952p.

Yu, D., Percival, P.W., Brodovitch, J.C., Leung, S.K., Kiefl, R.F., Venkateswaran, K., Cox, S.F.J., 1990. Structure and Intramolecular Motion of Muonium-Substituted Cyclohexadienyl Radicals. Chem. Phys. 142, 229-236. https://doi.org/10.1016/0301-0104(90)89084-4.